Analytical Biochemistry **271,** 70–80 (1999)
Article ID abio.1999.4129, available online at http://www.idealibrary.com on IDEAL®

The Choice of Reference Cell in the Analysis of Kinetic Data Using BIAcore

Raimund J. Ober*,[1] and E. Sally Ward*,†,[2]
*Cancer Immunobiology Center and †Center for Immunology, 6000 Harry Hines Boulevard, University of Texas Southwestern Medical Center at Dallas, Dallas, Texas 75235-8576

Received February 3, 1999

An important step in the analysis of sensorgram data for BIAcore experiments is the subtraction of reference cell data to remove the effects of the bulk shift on the sensorgram of interest. It is shown that this step can introduce errors in the measured kinetic constants. This phenomenon is investigated both theoretically and with experimental data. © 1999 Academic Press

Key Words: **kinetic constants; surface plasmon resonance; BIAcore; reference cell.**

The use of optical biosensors for the analysis of macromolecular interactions offers several advantages over more conventional approaches of affinity determination. First, the interacting components do not need to be labeled. Second, the amounts of material needed for analysis are relatively small. Third, multiple potential interactions can be analyzed in a relatively short time period.

In a BIAcore instrument soluble analyte is flowed over immobilized ligand and binding is monitored in real time using surface plasmon resonance (SPR)[3] technology. In the BIAcore 2000, flow of analyte over four flow cells on a sensor chip allows the simultaneous analysis of multiple interactions to be carried out with a single analyte injection (see, e.g., Refs. 3 and 8 for surveys of BIAcore methodology). One of the four flow cells is usually used as a reference surface. For protein–protein interactions this reference surface is either a flow cell treated with the coupling chemistry in the absence of added ligand or a flow cell coupled with a protein that is known not to interact with the analyte under analysis. Sensorgram data corresponding to the reference surface is then subtracted from that corresponding to the "binding" surface to remove effects of refractive index changes due to analyte injection and baseline drift.

Various artifacts are known to result in data that is difficult to interpret (see, e.g., 6). In order to reduce effects due to mass transport, rebinding, steric hindrance, and other transport-related artifacts, it is important to couple the ligand at low density to the flow cell (2, 4, 7, 9). This results in a low signal to noise ratio, which in turn can give rise to decreased accuracy of the estimated kinetic constants (5). Measurements of the association constant can be severely affected by inaccurate measurements of the analyte concentration.

In the current study we have addressed the effects of baseline drift and bulk shift subtraction on the accuracy of the estimates of the kinetic constants. An extensive analysis has been carried out to investigate this problem. The effects of subtracting data from different reference cells, obtained from the same analyte injection, have been investigated. The results indicate that significant errors can be introduced into the kinetic constants by the effects of random drifts in individual flow cells. Furthermore, these effects are exacerbated by increases in bulk shift and decreases in ligand coupling density.

MATERIALS AND METHODS

Preparation/Source of Proteins

Hen egg lysozyme (HEL) was purchased from Sigma (St. Louis, MO). D1.3 antibody (1) was purified from

[1] Permanent address: Center for Engineering Mathematics EC35, University of Texas at Dallas, Richardson, TX 75083.

[2] To whom correspondence should be addressed. Fax: (214) 648-1259.

[3] Abbreviations used: SPR, surface plasmon resonance; HEL, hen egg lysozyme; PBST, phosphate-buffered saline containing 0.01% Tween 20.

0003-2697/99 $30.00

hybridoma supernatants using protein G–Sepharose and standard methods.

Preparation of Sensor Chips

Flow cells of a CM5 chip were treated with a standard amine-coupling reagent (injecting 10 mM NaOAc, pH 4.8, instead of protein) or with amine-coupling reagents and D1.3 antibody. The coupling density of the D1.3 antibody was 270RU.

Data Collection

Experiments were run at 25°C (buffer only experiments) and 20°C (D1.3 antibody–HEL experiments) using programmed methods and the BIAcore control software. In experiments involving the HEL:D1.3 antibody interaction, HEL was injected at concentrations of 100, 10, and 1 nM in phosphate-buffered saline, pH 7.2, containing 0.01% (v/v) Tween 20 (PBST, pH 7.2). PBST (pH 7.2) was used as running buffer for all experiments, and analyte injections were carried out using the kinject command. Buffers were degassed and filtered through 0.2 μM cut-off Corning filters prior to use. Experiments were run with multiple repeats for each set of conditions, and flow rates of 5 and 80 μl/min were used. All experiments were preceded by extensive equilibration runs.

Data Processing

The data were analyzed using algorithms coded in the high-level programming language MATLAB. The optimization toolbox in MATLAB was used to implement a nonlinear search routine to fit the kinetic parameters to the association and dissociation data in a least squares sense. For each sensorgram a fit was carried out for the association and dissociation phases following zero adjustment and subtraction of reference cell sensorgrams. The time axes for the sensorgrams collected in the four flow cells were adjusted to compensate for the varying time delays that are due to the differing lengths of the flow paths. These algorithms were used rather than the manufacturer's software since they allowed for a more efficient and uniform processing of the large data sets that were used in this study. A comparison of our implementation of the estimation algorithms with those of the manufacturer showed that they were at least equally accurate and appear to have fewer convergence problems.

For the simulation studies, data were simulated using the integrated form of Eq. [1] and independent Gaussian noise was added. The analysis of the simulated data was carried out in a way analogous to that used for the analysis of the experimental data. More precise details of the simulations are given in the legends corresponding to the figures.

RESULTS

Rationale

In order to measure the kinetic constants by BIAcore first (Step 1) buffer is flowed over the chip on which the protein is coupled. This is followed (Step 2) by flowing the analyte over the chip. During this phase the association constant can be measured. Immediately following the analyte injection (Step 3) buffer is again flowed over the chip. During this step of the experiment the dissociation constant of the interaction can be determined by measuring the rate of decrease of the concentration of the analyte–ligand complex on the chip. The injection of analyte, i.e., Step 2, will typically lead to a bulk shift, i.e., a significant change in signal which is mainly due to the change in refractive index of the analyte in comparison with the buffer. This bulk shift is also observed in a reference cell in which no protein or a protein which does not bind to the analyte is coupled. The sensorgram corresponding to this reference cell is then subtracted from the sensorgrams of the flow cells in which the actual interaction is being measured. This procedure can also subtract out other artifacts in the data such as baseline drift. In this paper we investigate with both theoretical and experimental means the effect of imperfections in this approach on the accuracy of the estimates.

The interactions that we study are assumed to obey the following kinetic equations of a 1:1 interaction

$$\frac{dR}{dt} = k_{on}C(R_{max} - R) - k_{off}R, \qquad [1]$$

where R is the measured signal in resonance units (RU), k_{on} is the association constant, k_{off} is the dissociation constant, R_{max} the maximum analyte-binding capacity in RU, and C is the concentration of the analyte that is flowed over the chip during the association phase. During the association phase (Step 2 of the experiment) the concentration term C is assumed to be constant. Before the association phase (Step 1) and during the dissociation phase (Step 3) the concentration is assumed to be 0. In fact, this equation can be easily solved analytically both for the association and for the dissociation phase (see below).

As discussed above, the sensorgram S, the measured signal, is made up of a contribution R which is due to the changing concentration of the ligand–analyte complex on the chip and the bulk shift B which possibly includes other effects such as baseline drift, i.e.,

$$S(t) = R(t) + B(t), \quad t \geq 0.$$

The part of the signal that is of interest is R, i.e., the contribution due to the changing concentration of the ligand–analyte complex. It is therefore important to remove the contribution due to the disturbance B. In order to do this, in a standard experiment one of the four flow cells will not have any ligand or an irrelevant ligand coupled to it. The signal B_1 in this reference cell is then measured and subtracted from the signal S. It is usually assumed that B_1 equals B and therefore that the subtracted signal

$$S_{\text{sub}} = S - B_1 = R + B - B_1$$

in fact equals S. The purpose of this paper is to examine both theoretically and experimentally to what extent this assumption is justified and what the effect is on the measured kinetic constants if there is a nonzero error

$$\Delta B = B - B_1.$$

This study has been carried out by assessing the effects of subtracting different reference cell data corresponding to different uncoupled flow cells within the same chip.

Buffer Injections over Uncoupled Flow Cells

There is a certain arbitrariness concerning the choice of reference cell. The objective of the first set of experiments was to assess the extent of variability for data obtained from four identical flow cells within the same sensor chip. To this end simple experiments were conducted in which buffer was injected over a CM5 sensor chip for which all cells were treated with the amine coupling chemistry in the absence of protein ligand; i.e., buffer only was used as the "ligand" in the coupling cycle. Buffer was then injected (using kinject) over all flow cells using aliquots of the running buffer. In addition, one series of runs was carried out with twofold diluted running buffer to assess the effects of intentionally introducing large bulk shifts (in this case, downwards) in the data. The results of 2 of a total of 36 experiments are shown in Figs. 1 and 2. It follows very clearly that there can be considerable variability between the sensorgrams of the bulk shifts in the four channels, even when the running buffer is matched with the injected buffer. However, this variability becomes even more marked when larger bulk shifts are introduced, e.g., by using buffer that is more dilute than the running buffer (Fig. 2).

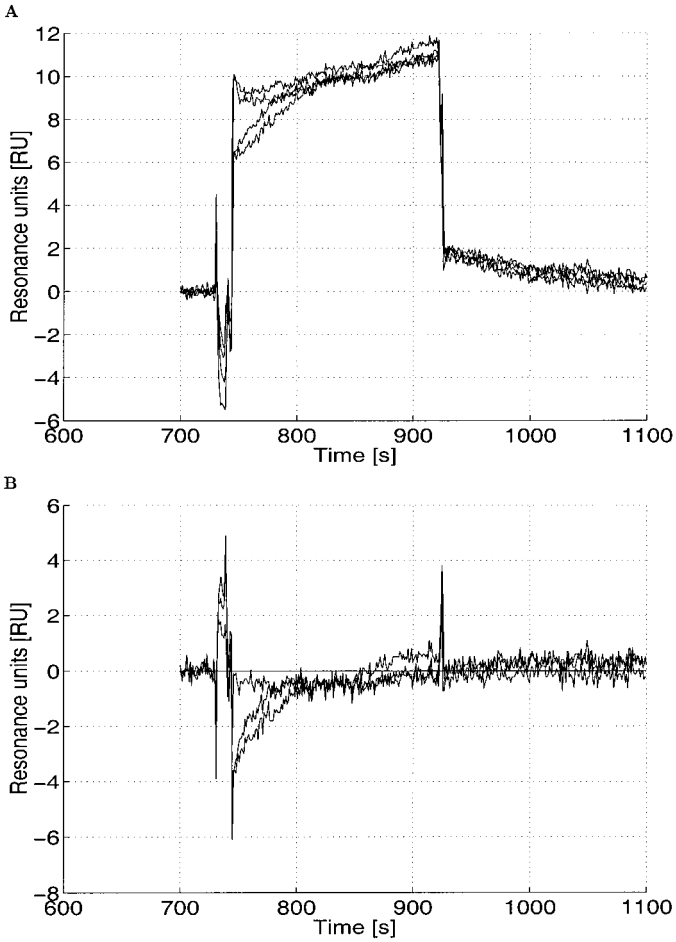

FIG. 1. (A) A representative set of sensorgrams (flow rate: 80 μl/min) from the four flow cells of a buffer (PBST, pH 7.2) injection over an uncoupled chip. The data were zero adjusted. The injected buffer was an aliquot of the running buffer. (B) Same data as in (A) after background subtraction using the data recorded in flow cell 1.

It should be noted that even if buffer is injected from an aliquot of the running buffer, a bulk shift is seen (Fig. 1). Following subtraction of data for one of the flow cells from that corresponding to the three other "identical" flow cells, the resulting signals (Fig. 1) show significant drifts and offsets, especially during the association phase.

Figure 2B shows the buffer runs of Figure 2A after the sensorgram of flow channel 1 has been subtracted. A significant residual signal level during the dissociation phase is shown in Figure 2C.

Effects of Deterministic Errors on the Estimated Kinetic Constants

In this subsection a theoretical study is carried out to investigate the influence of the above mentioned disturbances on the accuracy of the estimated kinetic constants.

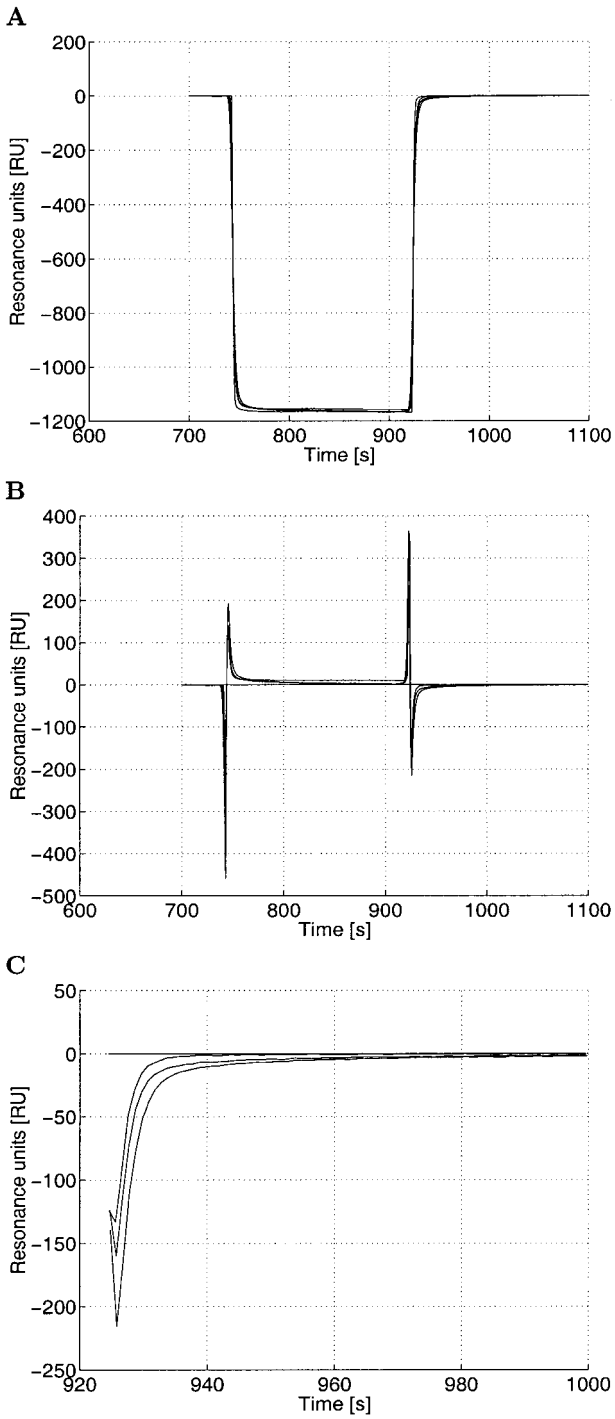

FIG. 2. (A) An experiment analogous to that shown in Fig. 1. In this case the flow rate was changed to 5 μl/min. The buffer was a twofold dilution of the running buffer, which resulted in a significant downward bulk shift. The time axis of the various flow cells was also adjusted to compensate for the differing delays which occur since the lengths of flow paths differ slightly for the different flow cells. (B) Data of (A) after subtraction of signal in flow cell 1. (C) Excerpt of (B) to show the dissociation phase.

Dissociation Constant

The dissociation signal of an experiment governed by the kinetic model [1] is given by

$$\mathrm{diss}(t) = ce^{-k_{\mathrm{off}}t}, \quad t \geq 0,$$

where c is a positive constant and k_{off} is the dissociation constant. A method to estimate the dissociation constant k_{off} is to differentiate the dissociation signal and to use linear regression to determine k_{off}. In practice this is rarely done. However, for the idealized study of this section in which we assume that no noise is present, this approach provides an easy way to analyze the estimation process. The signal diss differentiated at 0 is

$$\mathrm{diss}'(0) = \frac{d}{dt}\,\mathrm{diss}(t)\big|_{t=0} = -k_{\mathrm{off}}ce^{-k_{\mathrm{off}}t}\big|_{t=0} = -k_{\mathrm{off}}\mathrm{diss}(0).$$

An estimate $\hat{k}_{\mathrm{off}}$ of the dissociation constant k_{off} is then given by

$$\hat{k}_{\mathrm{off}} = -\frac{\mathrm{diss}'(0)}{\mathrm{diss}(0)}. \qquad [2]$$

Under the current assumptions we have that the estimate yields the correct constant, i.e., $\hat{k}_{\mathrm{off}} = k_{\mathrm{off}}$. This result is an idealized form of many of the other methods that are being employed to estimate the dissociation constant.

The topic of this paper is to analyze the influence of the error ΔB in the signal on the accuracy of the estimates of the kinetic constants. It is therefore assumed that the dissociation signal is given by

$$\mathrm{diss}(t) = ce^{-k_{\mathrm{off}}t} + \Delta B(t), \quad t \geq 0,$$

where the only assumption on the disturbance term ΔB is that it is differentiable at 0. If we apply the estimation procedure of Eq. [2], we obtain

$$\hat{k}_{\mathrm{off}} = -\frac{\mathrm{diss}'(0)}{\mathrm{diss}(0)} = \frac{k_{\mathrm{off}}c - \Delta B'(0)}{c + \Delta B(0)}. \qquad [3]$$

Clearly, if the disturbance term and its derivative are zero at time $t = 0$ then the correct constant is estimated.

Limiting situations. For fixed disturbance term it follows that

$$\hat{k}_{\mathrm{off}} \to k_{\mathrm{off}},$$

as c increases towards infinity, irrespective of the disturbance term. The implication is that even in the presence of a disturbance term its influence decreases as the size of the underlying signal increases. In contrast, as c decreases to 0 we have for a given disturbance component that

$$\hat{k}_{\text{off}} \to \frac{\Delta B'(0)}{\Delta B(0)}.$$

This shows that as the signal level decreases the estimated off-rate converges to a value that is independent of the dissociation constant.

Error analysis. The relative error between the estimated dissociation constant $\hat{k}_{\text{off}}$ and k_{off} is given by

$$\left|\frac{\hat{k}_{\text{off}} - k_{\text{off}}}{k_{\text{off}}}\right| = \left|\frac{\Delta B'(0) + \Delta B(0) k_{\text{off}}}{k_{\text{off}}(c + \Delta B(0))}\right|. \qquad [4]$$

Association Constant

The association signal of an experiment governed by the kinetic model [1] is given by

$$\text{ass}(t) = R_{\text{eq}}(1 - e^{-k_{\text{obs}}t}), \quad t \geq 0,$$

where R_{eq} is a positive constant that stands for the equilibrium level; i.e., R_{eq} equals the limit of the association signal as t approaches infinity, i.e., $R_{\text{eq}} = \text{ass}(\infty)$. The symbol k_{obs} stands for the "observed on-rate," which is given by $k_{\text{obs}} = Ck_{\text{on}} + k_{\text{off}}$, where C is the analyte concentration. In most cases k_{obs} is first estimated. The actual association constant k_{on} is then computed from k_{obs} given knowledge of C and k_{off}.

The observed on-rate can be estimated in a very similar fashion to the dissociation constant. For the time point $t_0 > 0$ we consider the derivative

$$\begin{aligned}\text{ass}'(t_0) &= k_{\text{obs}} R_{\text{eq}} e^{-k_{\text{obs}}t_0} \\ &= -k_{\text{obs}} R_{\text{eq}}(1 - e^{-k_{\text{obs}}t_0}) + k_{\text{obs}} R_{\text{eq}} \\ &= -k_{\text{obs}}\text{ass}(t_0) + k_{\text{obs}}\text{ass}(\infty).\end{aligned}$$

If we assume that $R_{\text{eq}} = \text{ass}(\infty)$ is known, then

$$k_{\text{obs}} = \frac{\text{ass}'(t_0)}{\text{ass}(\infty) - \text{ass}(t_0)} \qquad [5]$$

and therefore

$$k_{\text{on}} = \frac{1}{C}\left(\frac{\text{ass}'(t_0)}{\text{ass}(\infty) - \text{ass}(t_0)} - k_{\text{off}}\right). \qquad [6]$$

For the purposes of analyzing the influence of the above-mentioned phenomena on the estimates of the association constant, a disturbance component ΔB is added to the association signal,

$$\text{ass}(t) = R_{\text{eq}}(1 - e^{-k_{\text{obs}}t}) + \Delta B(t), \quad t \geq 0.$$

It is assumed that the disturbance term is differentiable at t_0 and that the limit $\Delta B(\infty)$ of the disturbance term as t approaches infinity is finite. From the expression for the on-rate estimate (Eq. [6]) we therefore have

$$\begin{aligned}\hat{k}_{\text{on}} &= \frac{1}{C}\left(\frac{\text{ass}'(t_0)}{\text{ass}(\infty) - \text{ass}(t_0)} - k_{\text{off}}\right) \\ &= \frac{1}{C}\left(\frac{k_{\text{obs}} R_{\text{eq}} e^{-k_{\text{obs}}t_0} + \Delta B'(t_0)}{R_{\text{eq}} e^{-k_{\text{obs}}t_0} + \Delta B(\infty) - \Delta B(t_0)} - k_{\text{off}}\right).\end{aligned}$$

Limiting situations. Analogously to the case of the dissociation constant, for a given disturbance ΔB, the estimated association constant $\hat{k}_{\text{on}}$ converges to the correct value k_{on} as the signal level increases to infinity, i.e.,

$$\hat{k}_{\text{on}} \to k_{\text{on}},$$

as $R_{\text{eq}} \to \infty$. As the signal level decreases to 0, we see that $\hat{k}_{\text{on}}$ converges to a value that is independent of the dissociation constant, i.e.,

$$\hat{k}_{\text{on}} \to \frac{1}{C}\left(\frac{\Delta B'(t_0)}{\Delta B(\infty) - \Delta B(t_0)} - k_{\text{off}}\right)$$

as $R_{\text{eq}} \to 0$.

Error analysis. The relative error between the estimated association constant $\hat{k}_{\text{on}}$ and k_{on} is given by

$$\left|\frac{\hat{k}_{\text{on}} - k_{\text{on}}}{k_{\text{on}}}\right| = \left|\frac{\Delta B'(t_0) - k_{\text{obs}}\Delta B(\infty) + k_{\text{obs}}\Delta B(t_0)}{k_{\text{on}} C(R_{\text{eq}} e^{-k_{\text{obs}}t_0} + \Delta B(\infty) - \Delta B(t_0))}\right|. \qquad [7]$$

Comparison of the Theoretical Results with Simulations

The formulas for the errors (Eqs. [4] and [7]) were derived using idealized assumptions which will not occur in practice when experimental data is analyzed. The basic assumption behind these derivations was that the value of the association/dissociation curve and its derivative are known at a particular point in time. Due to the presence of noise in experimental data this is of course not a valid assumption, and iterative search methods are employed to estimate the kinetic constants from longer data segments. These formulas can therefore only be expected to be an approximation

of the errors that are encountered in the analysis of experimental data. The purpose of the study that is carried out in this section is to investigate how accurate these formulas are if they are compared with estimates based on simulated data.

Figure 3A shows a comparison of the estimate of the dissociation constant based on Eq. [3] with the estimates that are obtained from the simulated data using an iterative search routine. Figure 3B shows a comparison of the error formula for the estimate of the dissociation constant with the errors that are encountered using the estimates obtained from the simulated data. Signal levels ranging from 5 to 100 RU are used for this simulated data since for protein–protein interactions this is a suitable signal level to minimize effects due to rebinding, mass transport (see discussion in the Introduction). Figure 4 shows the analogous results for the estimation of the association constant.

The disturbance terms that were used in the simulations (Figs. 3 and 4) in the current study were relatively small compared with the disturbance terms that can be encountered due to the bulk shift subtraction problems that were discussed above. In fact, the slope of the linear disturbance term was chosen to be slightly less than the limits set by the machine specifications for baseline drift, a phenomenon that is much less problematic than the bulk-shift-induced artifacts being discussed here. It should be pointed out, however, that both in the analytical derivation of the error estimates and in the nonlinear search routine a disturbance term was not included. Although at first this may appear to be inappropriate, there are a number of reasons for doing this. In a practical situation often only a short data segment can be used in the data analysis since longer segments often display artifacts, including rebinding phenomena. For short data segments the inclusion of drift terms provides notoriously unreliable estimates. Moreover, the type of disturbance terms that arise from the bulk shift subtraction effects usually cannot be described as linear functions.

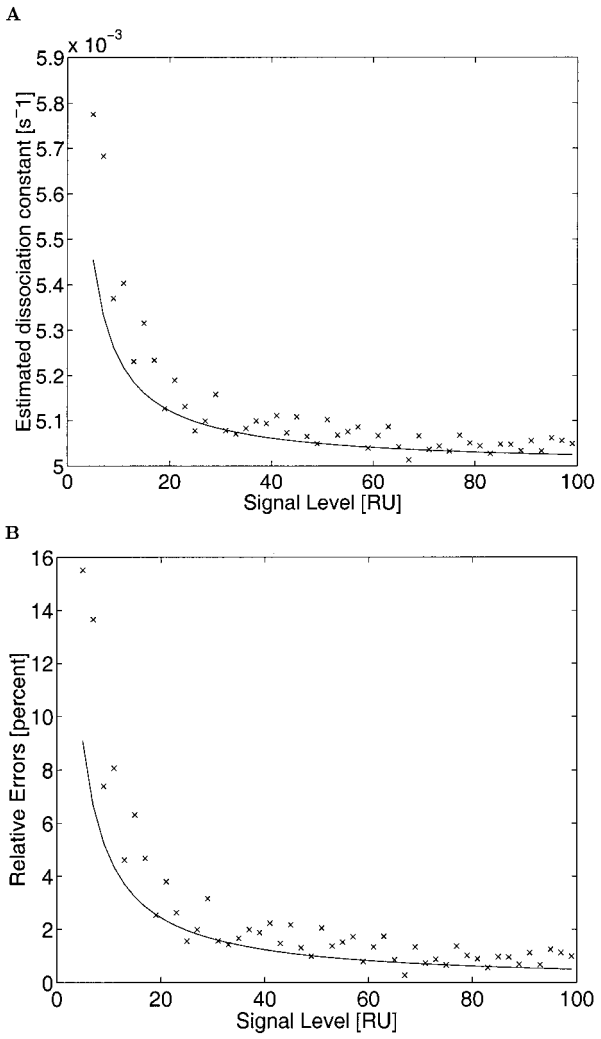

FIG. 3. (A) Estimated dissociation constants. The x-coordinate denotes the signal level, i.e., the starting point of the dissociation curve. Dissociation data was simulated with dissociation constant $k_{off} = 0.005\ s^{-1}$. Zero mean Gaussian noise of standard deviation 0.25 RU and a disturbance term $\Delta B(t) = -0.005t + 0.5$ (in RU) were added to the simulated dissociation curve. This level of drift is within the specification of the instrument. The dissociation constant was then estimated using a nonlinear search routine programmed in the high-level programming language Matlab. Each data point (x) is an average of four estimated dissociation constants for the particular signal level c. The data (—) show the estimated dissociation constant based on Eq. [3] for the given data. (B) Relative errors as percentages of the dissociation constant estimate. The data used are the same as those in (A). The data (x) show the relative errors as percentages corresponding to the estimates shown in (A). The data (—) show the estimated relative error based on Eq. [4] for the given data.

Effects of Different Experimental Reference Cell Data on the Analysis of a Simulated Sensorgram

In order to study the effects of bulk shift subtraction on the accuracy of the kinetic constants, the following analysis was carried out. A sensorgram was simulated and experimentally obtained bulk shift signals were added. The reason for carrying out this analysis was that in contrast to experimental data, in this situation the kinetic constants that need to be recovered are known. For the simulated data, a curve for an interaction of hypothetical on-rate of 1960 $M^{-1}s^{-1}$ and off-rate of 5×10^{-3} was generated ($R_{eq} = 20$ RU). Reference cell data were produced by injecting buffer over four uncoupled flow cells of a sensor chip using the BIAcore 2000 (Fig. 5). The buffer was injected from either capped or uncapped vials of aliquots of the running buffer. Each row of Fig. 5 shows a series of three injections from the same vial. Uncapped vials were intentionally used to assess the effects of buffer dehy-

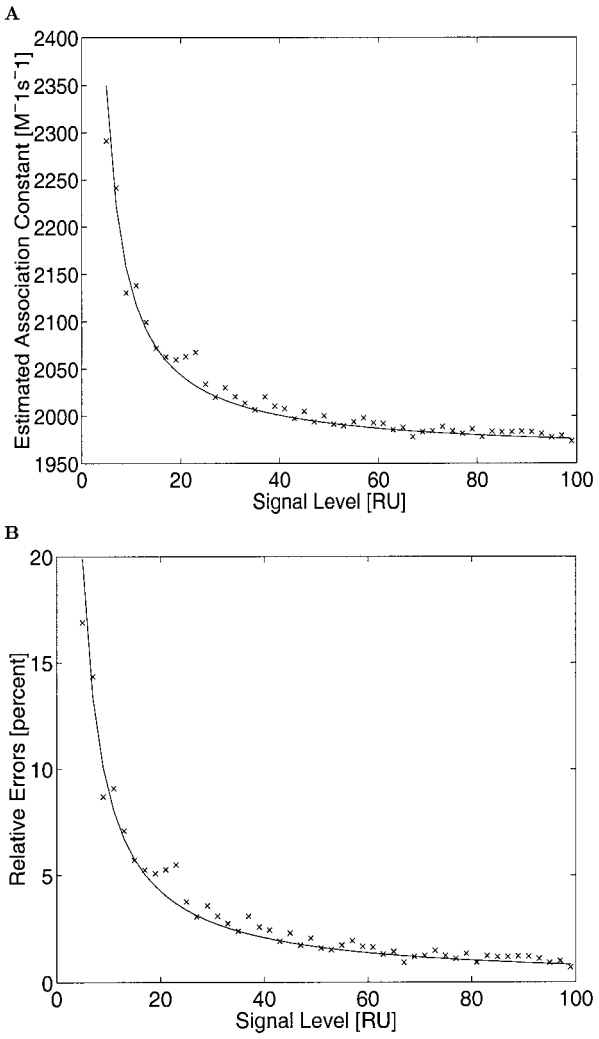

FIG. 4. (A) Data analogous to those in Fig. 3 displaying estimates of association constant based on Eq. [6] (—) and based on an iterative search method to determine the parameters from simulated data (x). The data were simulated analogously to the simulations described in the legend to Fig. 3. The association constant is k_{on} = 1960 M^{-1} s^{-1} and the observed association constant is k_{obs} = 0.103 s^{-1}. The term signal level here stands for the signal at equilibrium, i.e., R_{eq}. (B) Relative errors as percentages of the estimate of the association constant. The data used are the same as those in (A). The data (x) show the relative errors as percentages corresponding to the estimates shown in (A). The data (—) show the estimated relative error based on Eq. [7] for the given data. The term $\Delta B(\infty)$ in Eq. [7] was taken to be the linear drift evaluated at the last data point that was considered for the analysis ($\Delta(\infty)$ = 0.175 RU).

dration during the course of an experiment. Data from flow cell 4 was added to the simulated curve and reference cell data from flow cells 1, 2, and 3 were then subtracted. On and off rates were determined for each of these processed curves. A total of nine different sets of reference cell data sets (Fig. 5) was used. The sizes of the buffer signals vary considerably. The signals resulting from injections from the same uncapped vial (last row) are larger than those from the two capped vials (first two rows). However, once the cap of a vial has been broken due to an injection, the signals increase significantly (second and third columns of first two rows). The on- and off-rates for the processed data (i.e., simulated curves with real reference cell data subtracted) are shown in Figs. 6–8.

Both Fig. 7 and Fig. 8 show association constants for the various simulated data sets. The errors in Fig. 7 are significantly higher than those in Fig. 8. While the underlying data sets for both figures were identical, different segments of the association phases of the signals were chosen. The number of data points that were analyzed was identical in both cases. In Fig. 8 the data window was, however, shifted by +5 s. The effect of this shift was that much of the difference between the transients of bulk shifts had died down at the beginning of the data segment that was analyzed. This resulted in a much lower variability between the various data segments and hence in a lower scatter of the estimated association constants.

In another study (5) the effect of random noise in the measured sensorgrams on the estimated kinetic constants was investigated. It was shown that with the

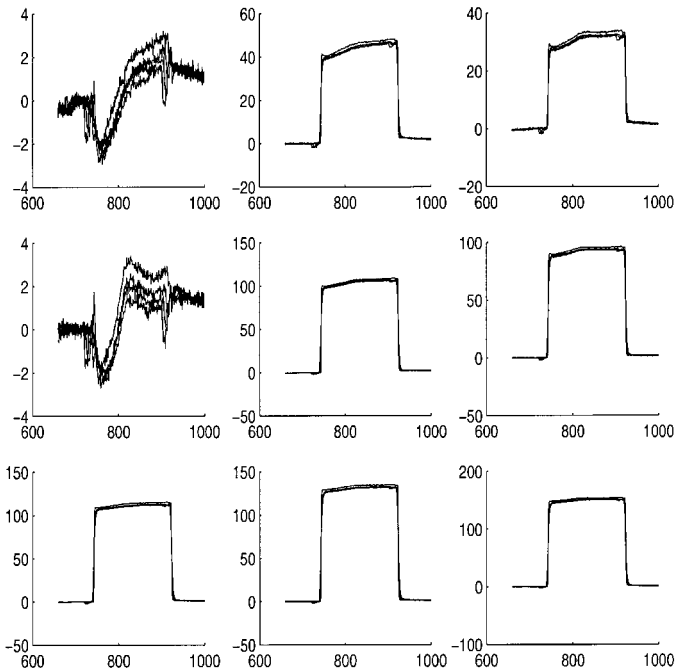

FIG. 5. Sensorgrams of buffer (PBST, pH 7.2) injection over uncoupled flow cells. The flow rate was 5 μl/min. The three sensorgrams in the first row show a sequence of three injections from the same capped vial. The second row of sensorgrams shows a repeat of the same experiment. The third row of sensorgrams is again a repeat experiment, but this time the vial for the buffer injections was not capped.

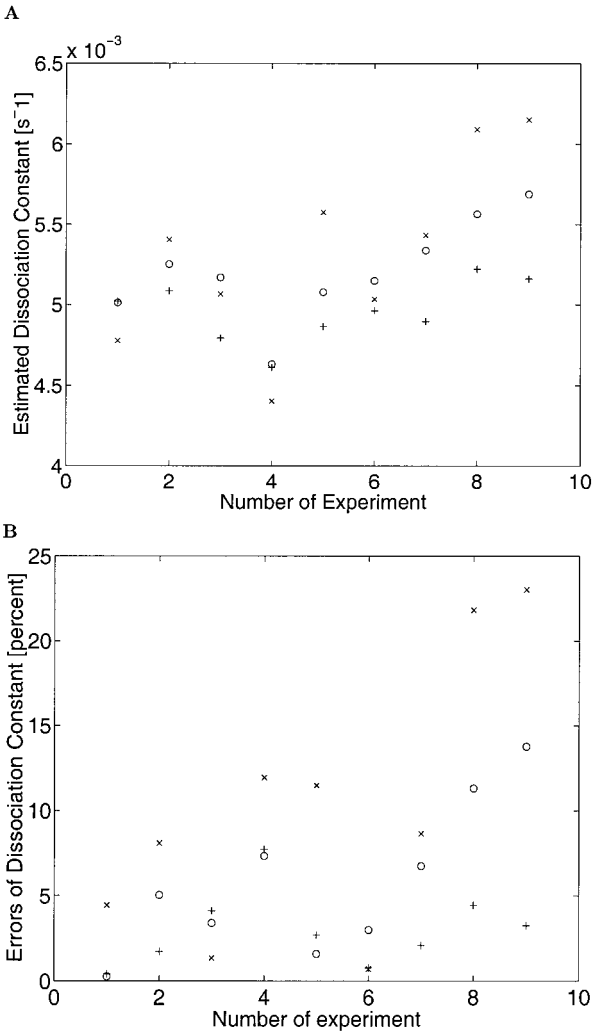

FIG. 6. (A) Estimated dissociation constants obtained from an analysis of simulated data with added/subtracted experimental bulk shifts. A sensorgram was simulated with dissociation constant $k_{off} = 5 \times 10^{-3}$ s^{-1}, association constant $k_{on} = 1960$ M^{-1} s^{-1}, concentration $C = 5 \times 10^{-5}$ M, and $R_{eq} = 20$ RU. To this sensorgram the nine data sets from flow cell four of the bulk shifts of Fig. 5 were sequentially added to obtain nine sensorgrams that have differing bulk shift components. The data sets from flow cells 1–3 of Fig. 5 are treated as data from three reference cells. To emulate what is typically done in the analysis of BIAcore data the data from these "reference cells" were subtracted from the data that were simulated to correspond to reference cell four. The resulting data were then analyzed. In this figure the estimated dissociation constants are shown. The data points (x) show the estimated dissociation constants when the bulk shift of flow cell 1 has been subtracted from the data corresponding to flow cell 4. The data points ○ and + indicate the estimates obtained after the subtraction of the bulk shifts of flow cell 2 and flow cell 3, respectively. (B) The relative errors as percentages of the estimated dissociation constants shown in (A).

estimation procedure that is being used (gradient based minimization of a least squares criterion) the standard deviation of the estimated kinetic constants is very close, if not identical, to the Cramer–Rao lower bound for which an analytical expression was given. In order to exclude the possibility that the scatter of the estimated kinetic constants in this study is solely due to the naturally occurring scatter of estimates based on noisy data, the lower bounds on the standard deviations were calculated for the current simulations. In our analysis bulk shifts were measured and therefore have the same random noise level as any measured data on the instrument. The analyzed data therefore also has a random noise component. The standard deviation of the dissociation constant due to the random noise in the data is predicted to be 10^{-4} s^{-1}. For the association constant the standard deviation due to noise is predicted to be less than 30 M^{-1} s^{-1}. Both numbers are small in comparison to the scatter in the

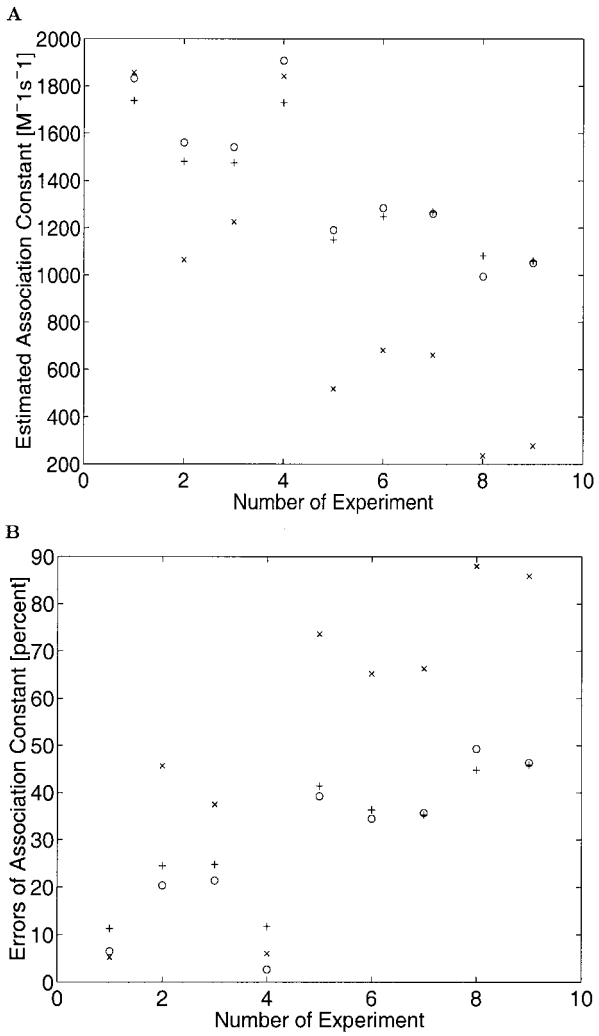

FIG. 7. (A) Estimated association constants of data described in the legend to Fig. 6. (B) The relative errors presented as percentages of the estimated association constants shown in (A).

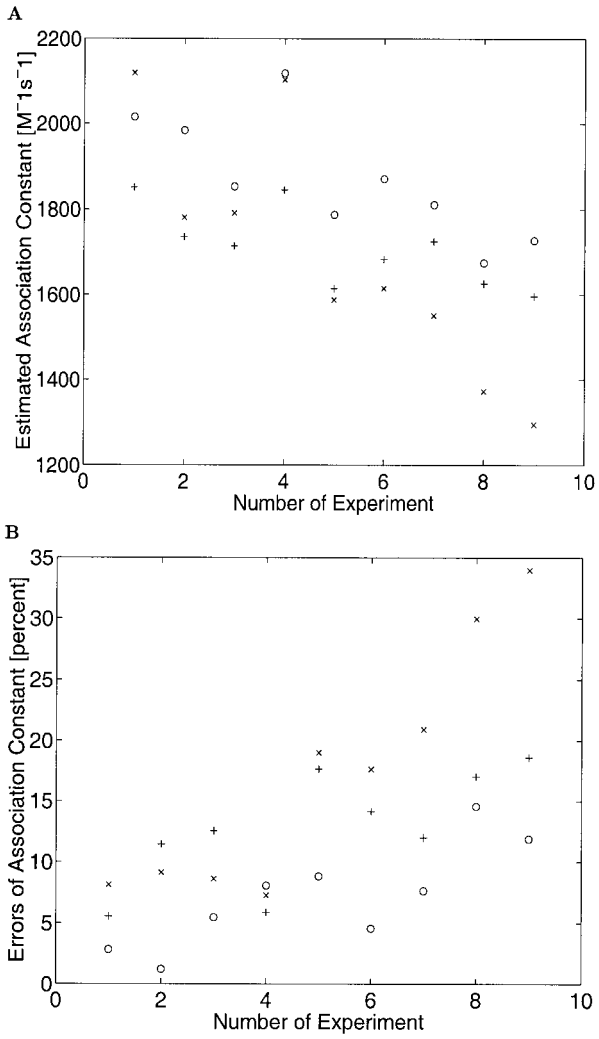

FIG. 8. (A) Estimated association constants of data described in the legend to Fig. 6. The difference between the estimated association constants shown here and the estimated association constants shown in Fig. 7 is that here the association constants were obtained by analysis of a data segment that was shifted by +5 s. (B) Shows the relative errors as percentages of the estimated association constants shown in (A). The errors obtained here are significantly lower than those obtained in Fig. 7.

estimated kinetic constants. It therefore follows that the observed scatter is unlikely to be due to the random noise component of the data, but should be attributed to disturbances introduced by the bulk shift subtractions.

Analysis of Experimental Data of HEL:D1.3 Antibody Interaction

Next, data from the analysis of the HEL:D1.3 antibody interaction was analyzed in an manner analogous to that shown in Figs. 5–7 for the simulated sensorgram. One flow cell of a sensor chip was coupled with D1.3 antibody and the remaining three flow cells were uncoupled. Data from the three uncoupled flow cells were then sequentially subtracted from the binding sensorgram and kinetic constants determined (Figs. 9 and 10). Data for two different flow rates are shown. For a flow rate of 5 μl/min, the on- and off-rates are generally lower (mean of 1.4×10^{-3} M^{-1} s^{-1} for the off-rate and mean of 6.9×10^{6} M^{-1} s^{-1} for the on-rate) than those obtained for a flow rate of 80 μl/min (mean of 2.1×10^{-3} M^{-1} s^{-1} for the off-rate and mean of 7.4×10^{6} M^{-1} s^{-1} for the on-rate), suggesting that even at the low ligand coupling density used in this experiment mass transport and rebinding effects are still operative. The R_{eq} values for this experiment were in the range of 5–12 RU. A comparison of the standard deviations for the estimated kinetic constants with the standard deviations that are predicted based on the noise content of the data (5) shows that the observed standard deviations cannot only be explained by the noise content of the data. This is further evidence that the background subtraction problems are indeed of significance.

DISCUSSION

The data in this report show that reference cell choice can result in significant variability in the kinetic constants that are obtained from BIAcore analyses. These effects become particularly marked at low signal levels and are due to irreproducibility of data obtained from reference flow cells within the same chip. The analysis of simulated data indicates that the effects are decreased if data are generated whose signal levels are high in comparison to the disturbances that are encountered. However, it is well known that data with high signal levels can have artifacts due to the presence of mass transport effects and rebinding (2, 4, 7, 9). Furthermore, at very high ligand coupling densities where the reference cell effects become negligible, steric hindrance will also adversely affect the reliability of the data. To obtain data that do not suffer from these artifacts, it is therefore essential to design experiments with low coupling densities.

Detailed analysis of buffer injections over “blank” reference flow cells indicates that there is variability in the data obtained from individual flow cells within the same chip. Although it is preferable to use a “nonbinding” protein coupled to a flow cell at the same density as the ligand which binds as a reference cell in SPR experiments, the use of blank reference cells in the current study gives estimates of the extent of the error that can be introduced by reference cell subtraction. In fact, larger errors might be expected if analogous experiments were carried out with protein-coupled refer-

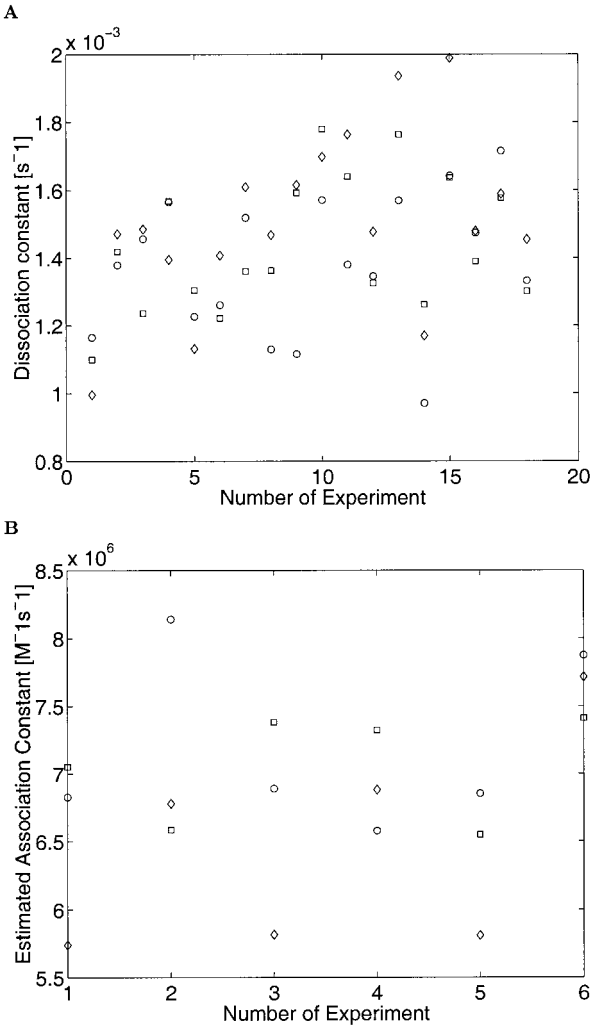

FIG. 9. (A) The estimated dissociation constants for 18 separate experiments are shown. In these experiments flow cell 4 of a chip was coupled with D1.3 antibody. The remaining three flow cells were left uncoupled. Eighteen experiments were conducted in which hen egg lycosyme (HEL) was injected. Three concentrations were used (100, 10, and 1 nM). For each concentration, six experiments were carried out. Vials containing the analyte were capped and three successive injections were taken from the same vial. The experiments were conducted at a flow rate of 5 lμl/min. In order to remove the bulk shift from the interaction data, reference cell data acquired in flow cells 1–3 was subtracted (after suitable adjustment of the time axes of the sensorgrams to compensate for differing lengths of the flow paths among the various flow cells). The data points (◇) correspond to the estimated dissociation constants after reference cell data in flow cell 1 was subtracted. The subtraction of reference cell data acquired in flow cells 2 and 3 lead to the estimated dissociation constants marked by □ and ○, respectively. The signal levels were between 5 and 12 RU. The bulk shifts were in the range 2–25 RU. (B) Estimated associations constants for data discussed in (A) for 10 nM injections.

ence cells due to variations in the amounts of protein coupled to individual flow cells (most likely due to pipetting errors). Surprisingly, even injection of buffer that is identical to the running buffer can result in bulk shifts of up to about 100 RU. The irreproducibility between flow cells becomes more marked as the bulk shift is increased, for example, by using a different buffer to the running buffer. Although this situation can usually be avoided, this is not always the case. For example, when low-affinity interactions or the pH dependence of the kinetics of an interaction are being investigated larger bulk shifts are by necessity introduced. In this respect, effects of buffer pH changes on the dextran matrix of the chips have been described previously (2). In addition, the analysis of low-affinity interactions necessitates the use of high analyte concentrations, which results in large bulk shifts. The bulk shift appears to increase significantly once the cap of the vial is punctured, suggesting that the use of

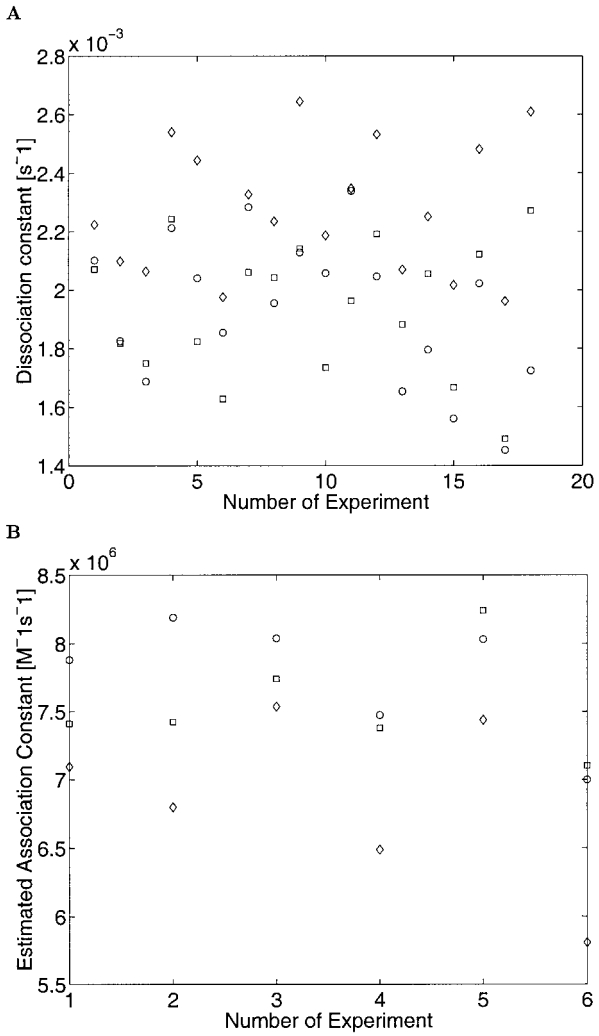

FIG. 10. (A) Estimated dissociation constants for a data set analogous to that described in the legend to Fig. 9 but acquired with a flow rate of 80 lμl/min. (B) Estimated association constants for data discussed in (A) for 10 nM injections.

individual capped vials for each injection may be preferable to the use of the same vial for multiple injections. Extensive equilibration of the chip with running buffer appears to reduce some of the phenomena that we discussed, but no evidence has been obtained that equilibration removes them.

In the current study both experimental and simulated data have been analyzed. Simulations of the effects of drifts on a simulated binding curve indicate that there is a strong dependence of the errors on the signal level. The drift was chosen to be within the manufacturer's specifications for the BIAcore 2000. Below a signal of about 20 RU, the estimates of the kinetic constants become unreliable. Experimental reference cell data are subtracted from either a simulated sensorgram or sensorgrams obtained from the analysis of the HEL:D1.3 antibody interaction. For both types of interaction curves, subtraction of reference cell data corresponding to different flow cells within the same chip introduces significant variation in the kinetic constants that are extracted from the binding sensorgrams. Other errors can be introduced into the constants obtained from SPR data due, for example, to the following: inaccurate protein (analyte) concentration estimation, ligand heterogeneity induced during coupling, steric hindrance effects, mass transport, and rebinding effects. How these errors affect the kinetic constants, and the effects relative to the errors due to reference cell subtraction described here, will be dependent on the particular experimental set up. However, there is clearly a balance between using higher coupling densities to reduce the errors introduced by reference cell subtraction and minimizing the ligand density to decrease mass transport and rebinding.

A further concern is the effect of reference cell data subtraction on model selection, where curve fitting to different interaction models is carried out. Clearly, artifacts in the data could bias fitting to one model in preference to another. Furthermore, since model fitting to kinetic data should by necessity be carried out using low ligand densities, the reference cell effects may be significant.

The data in this study indicates that it is very important to obtain a reasonable appreciation of the nature of the bulk shifts in the particular experiment. Since the behavior of the bulk shifts during the rise and decay time appears to differ between the four flow cells, even after subtraction, large perturbations with long transient behavior can remain. In analyzing the acquired data, it is particularly important that the data window used to determine the kinetic constants is chosen to minimize the influence of these phenomena. The analytical formulae presented (Eqs. [4] and [7]) can provide guidance for the design of experiments so as to reduce the influence of these artifacts on the measured kinetic constants.

ACKNOWLEDGMENTS

We are indebted to D. Eaken for expert technical assistance. This research was supported in part by the NSF (DMS 9803186/DMS 9501223) and the NIH (AI/NS 42949).

REFERENCES

1. Amit, A. G., Mariuzza, R. A., Phillips, S. E. V., and Poljak, R. J. (1986) *Science* **233,** 747–753.
2. Karlsson, R., and Fält, A. (1997) *J. Immunol. Methods,* 121–133.
3. Morton, T., and Myszka, D. (1998) *Methods Enzymol.* **295,** 268–294.
4. Myszka, D. G., Morton, T. A., Doyle, M. L., and Chaiken, I. M. (1997) *Biophys. Chem.* **64,** 127–137.
5. Ober, R., and Ward, E. S. (1998) Submitted for publication.
6. O'Shannessy, D. J., and Winzor, D. J. (1996) *Anal. Biochem.* **236,** 275–283.
7. Schuck, P. (1996) *Biophys. J.* **70,** 1230–1249.
8. Schuck, P. (1997) *Curr. Opinion Biotechnol.* **8,** 498–502.
9. Schuck, P., and Minton, A. P. (1996) *Anal. Biochem.* **240,** 262–272.